J|A|C|S
ARTICLES
Published on Web 11/20/2002

Hydrogen Adsorption on the Indium-Rich Indium Phosphide (001) Surface: A Novel Way to Produce Bridging In−H−In Bonds

K. Raghavachari,[§] Q. Fu,[†] G. Chen,[†] L. Li,[‡] C. H. Li,[†] D. C. Law,[†] and R. F. Hicks*,[†]

Contribution from the Chemical Engineering Department, University of California, Los Angeles, California 90095, Department of Physics, University of Wisconsin, Milwaukee, Wisconsin 53201, and Materials Research, Agere Systems, Murray Hill, New Jersey 07974

Received March 7, 2002

Abstract: The indium phosphide (001) surface provides a unique chemical environment for studying the reactivity of hydrogen toward the electron-deficient group IIIA element, indium. Hydrogen adsorption on the In-rich $\delta(2 \times 4)$ reconstruction produced a neutral, covalently bound bridging indium hydride. Using vibrational spectroscopy and ab initio cluster calculations, two types of bridging hydrides were identified, a $(\mu\text{-H})In_2$ and a $(\mu\text{-H})_2In_3$ "butterfly-like" structure. These structures were formed owing to the large thermodynamic driving force for adsorption of H atoms on solid-state indium dimers.

I. Introduction

Electron-deficient group IIIA hydrides (M−H, where M = B, Al, Ga, In, or Tl) have been the subject of extensive studies, primarily because they contain three-center two-electron (3c-2e) bridging hydrogen bonds.[1−14] Many discoveries have been made in preparing these compounds and characterizing their chemical and structural properties. More than 25 polyhedral boranes (B_nH_m with n varying from 1 to 20) have been synthesized over the years.[2,3] By contrast, structures formed with the heavier elements are much fewer in number. Aluminum hydride exists only as a polymeric solid of $(AlH_3)_n$,[6] while digallane (Ga_2H_6) has been synthesized in an inert-gas matrix at cryogenic temperatures.[7,8]

It is even more difficult to prepare compounds with indium hydride bonds. Pullumbi et al. synthesized and characterized indane, InH_3, in low-temperature matrix isolation experiments.[9] Several other compounds with terminal In−H bonds have been prepared by incorporating bulky ligands into the organometallic molecules, such as in $[Li(thf)_2]-[\{(Me_3Si)_3C\}_2In_2H_5]$, $InH\{2\text{-}Me_2NCH_2(C_6H_4)\}_2$, and $Me_2InB_3H_8$.[10] Most attempts to produce compounds with bridged hydrogen bonds have been unsuccessful, except in the case of the salts $K[H\{In(CH_2CMe_3)_3\}_2]$ and $[Li(tmeda)_2]-[Me_3In-H-InMe_3]$, where the indium exists in a negatively charged complex.[10]

We have developed an alternative approach to studying hydrogen bonds to electron-deficient group IIIA elements. Atomic hydrogen is adsorbed onto the surface of a group IIIA-rich III−V compound semiconductor, and the properties of the M−H bonds are examined by experimental and theoretical means.[15−19] The (001) plane of compound semiconductors consists of alternating layers of group III and V atoms. The surface may be terminated with either one of these elements, depending on the preparation method. In the ideal case, each atom exposed on the surface has two dangling bonds. However, to minimize the total surface energy, one of the dangling bonds is eliminated by forming dimers between neighboring atoms.[20] On group IIIA-rich surfaces, a high concentration of metal dimers is observed. Adsorption of hydrogen atoms on these sites leads to the formation of stable metal hydrides at room temperature. Thus far, we have characterized the gallium hydrides generated on the different reconstructions of GaAs (001).[17]

In this work, we report on hydrogen bond formation on the indium-rich InP (001) surface. Two types of bridging hydrides

* To whom correspondence should be addressed. E-mail: rhicks@ucla.edu.
† University of California.
‡ University of Wisconsin.
§ Agere Systems.

(1) Taylor, M. J.; Brothers, P J. In *Chemistry of Aluminum, Gallium, Indium and Thallium*; Downs, A. J., Ed.; Blackie: Glasgow, 1993; p 111.
(2) Cotton, F. A.; Wilkinson, G. *Advanced Inorganic Chemistry*; John Wiley & Sons: New York, 1988.
(3) Greenwood, N. N. *The Chemistry of Boron*; Pergamon Press: Oxford, 1975.
(4) Lawrence, S. H.; Wermer, J. R.; Boocock, S. K.; Banks, M. A.; Keller, P. C.; Shore, S. G. *Inorg. Chem.* **1986**, *25*, 367.
(5) Downs, A. J.; Pulham, C. R. *Chem. Rev.* **1994**, *23*, 175.
(6) Browser, F. M.; Matzek, N. E.; Reigler, P. F.; Rinn, H. W.; Roberts, C. B.; Schmidt, D. L.; Snover, J. A.; Terada, K. *J. Am. Chem. Soc.* **1976**, *98*, 2450.
(7) Downs, A. J.; Goode, M. J.; Pulham, C. R. *J. Am. Chem. Soc*. **1989**, *111*, 1936.
(8) Pulham, C. R.; Downs, A. J.; Goode, M. J.; Rankin, D. W. H.; Robertson, H. E. *J. Am. Chem. Soc.* **1991**, *113*, 5149.
(9) Pullumbi, P.; Bouteiller, Y.; Manceron, L.; Mijoule, C. *Chem. Phys*. **1994**, *185*, 25.
(10) Hibbs, D. E.; Hursthouse, M. B.; Jones, C.; Smithies, N. A. *Organometallics* **1998**, *17*, 3108 and references therein.
(11) Hunt, P.; Schwerdtfeger, P. *Inorg. Chem.* **1996**, *35*, 2085.
(12) Bennett, F. R.; Connelly, J. P. *J. Phys. Chem.* **1996**, *100*, 9308.
(13) Duke, B. J.; Liang, C.; Schaefer, H. F. *J. Am. Chem. Soc*. **1991**, *113*, 2884.
(14) Fu, Q.; Negro, E.; Chen, G.; Law, D. C.; Li, C. H.; Hicks, R. F.; Raghavachari, K. *Phys. Rev. B* **2002**, *65*, 075318.
(15) Qi, H.; Gee, P. E.; Hicks, R. F. *Phys. Rev. Lett.* **1994**, *72*, 250.
(16) Li, L.; Han, B.-K.; Fu, Q.; Hicks, R. F. *Phys. Rev. Lett.* **1999**, *82*, 1879.
(17) Hicks, R. F.; Qi, H.; Fu, Q.; Han, B. K.; Li, L. *J. Chem. Phys.* **1999**, *110*, 10498.
(18) Fu, Q.; Li, L.; Hicks, R. F. *Phys. Rev. B* **2000**, *61*, 11034.
(19) Fu, Q.; Li, L.; Li, C. H.; Begarney, M. J.; Law, D. C.; Hicks, R. F. *J. Phys. Chem. B* **2000**, *104*, 5595.
(20) Pashley, M. D. *Phys. Rev. B* **1989**, *40*, 10481.

are observed, a (μ-H)In_2 and a (μ-H)$_2In_3$ structure. It is found that In−H−In bond formation is strongly favored owing to the exothermic reaction between gas-phase hydrogen atoms and three-fold-coordinated indium.

II. Experimental Section

Indium phosphide films, 0.5 μm thick, were grown on InP (001) substrates by organometallic vapor-phase epitaxy.[21] The following optimized conditions were used during growth: 600 °C, 20 Torr of hydrogen, 6.5×10^{-4} Torr of tri-isopropylindium (TIPIn), 0.13 Torr of *tert*-butylphosphine (TBP) (V/III ratio of 200), and a total flow rate of 2.5 L/min at 25 °C and 760 Torr. After shutting off the TIPIn supply, the TBP and hydrogen flows were maintained until the samples were cooled to 300 and 40 °C, respectively. Then the crystals were transferred directly to an ultrahigh vacuum chamber without air exposure. In a vacuum, the samples were annealed in 1×10^{-5} Torr of phosphine for 30 min at 500 °C to obtain the $\delta(2 \times 4)$ reconstruction.[21] After cooling the samples to 25 °C, the surface structure was characterized by low-energy electron diffraction (LEED) and scanning tunneling microscopy (STM). The latter images were obtained of the filled states at a sample bias of −3.0 V and a tunneling current of 0.5 nA.

The infrared spectra were recorded by multiple internal reflections through a trapezoidal InP crystal, $40.0 \times 10.0 \times 0.64$ mm^3. This crystal provided for 31 reflections off the front face. Two substrate orientations were examined: one with the long crystal axis parallel to the [$\bar{1}$10] direction and one with the long crystal axis parallel to the [110] direction. Hydrogen was dosed into the chamber at 5×10^{-7} Torr and dissociated to atoms by a tungsten filament located 4 cm away from the sample face. The flux of H atoms relative to H_2 molecules was estimated to be ~0.1%.[17] The surface was saturated after dosing hydrogen for 30 min (900 L H_2). Vibrational spectra were collected before and during hydrogen adsorption with a BIO-RAD FTS-40A spectrometer. These spectra were recorded at 8 cm^{-1} resolution and by co-adding 1024 scans. The spectra presented in this report show the change in reflectance (per reflection) that results from taking the ratio of the sample spectrum with a full coverage of hydrogen to that of the clean surface.

III. Theoretical Methods

The quantum chemistry calculations were performed on the idealized In_7P_8 structures shown in Figure 1. Cluster **1** contains two side-by-side indium dimers attached to eight "bulk" P atoms and three "bulk" In atoms. Cluster **2** contains a single indium dimer adjacent to an In atom in the same row. These species are tethered to eight "bulk" P atoms and four "bulk" In atoms. The second structure allows us to examine the effects of interacting bridging hydrides. To simulate hydrogen adsorption on the indium-rich $\delta(2 \times 4)$ reconstruction, hydrogen was added to the two In_7P_8 clusters, and ab initio calculations were performed to determine the optimum configurations. For hydrogen adsorption on the phosphorus-rich InP surface, the reader is referred to ref 14.

Typically, the truncated bulk bonds in the cluster models are terminated with hydrogen atoms to eliminate artifacts due to excess spin or charge. While such a treatment is appropriate for covalent materials such as silicon, it is not valid for indium phosphide due to the presence of three covalent bonds and one dative bond around each In or P atom. While a truncated covalent bond can be terminated with hydrogen, a different treatment is needed in the latter case. A logical approach for a dative In−P bond is not to truncate with H but to leave the In and P atoms three-fold coordinated (with the phosphorus carrying the pair of electrons). However, in our previous work on P-rich surfaces,[14] we found that three-fold coordinated In atoms are reactive and lead to unphysical bridging interactions. A more realistic model

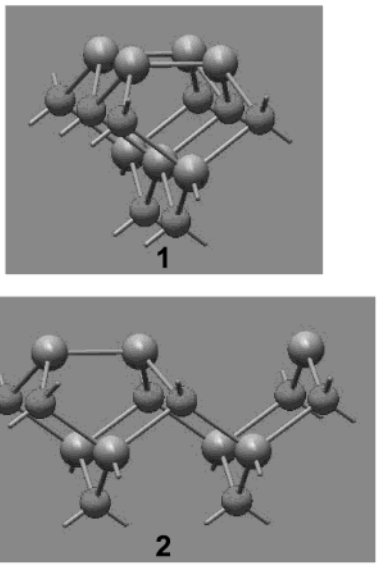

Figure 1. Models of the cluster backbones used to simulate hydrogen adsorption on indium dimers.

was found by datively bonding phosphine to the indium atoms, thereby maintaining tetra-coordination for all bulk In atoms on the cluster.

In the current work on the indium-rich surface, the corresponding procedure would have been to construct a cluster with InH_3 molecules datively bound to the second-layer phosphorus atoms. However, we found that neither the structure nor the vibrational frequencies changed significantly with this modification, and we decided to adopt the simpler model where the three-fold coordinated P atoms are left with their lone pairs of electrons. To achieve the proper valence configuration following hydrogen adsorption, three of the second layer phosphorus atoms are terminated with lone pairs, while the remainder of the bulk In and P atoms are truncated with hydrogen. The hydride chemistry of the $\delta(2 \times 4)$ InP (001) surface is simulated by adding hydrogen atoms to the terminal and bridging sites on the top-layer indium dimers.

The Gaussian98 quantum chemistry suite was used to optimize the structure of each $In_7P_8H_z$ cluster and predict its vibrational properties. These calculations were made utilizing density functional theory with the Becke three-parameter exchange functional and the Lee−Yang−Parr correlation functional (B3LYP). We chose the (18s/14p/9d)/[6s/5p/3d] contracted basis set for indium, the Dunning−Huzinaga (11s/7p/1d)/[6s/4p/1d] contracted basis set (D95**) for phosphorus, the D95** polarized double-ζ basis set for the surface hydrogen atoms, and the D95 double-ζ basis set for the terminating hydrogen atoms. The third-layer In and fourth-layer P atoms, along with their attached H atoms, were frozen along tetrahedral directions (In−P = 2.54 Å, In−H = 1.76 Å, P−H = 1.42 Å), while the remaining atoms were fully allowed to relax. The frozen degrees of freedom were removed in the force constant analysis, and no negative vibrational frequencies were observed for the final structures.

In our previous work on hydrogen adsorption on silicon and on P-rich indium phosphide, we have successfully applied a single frequency shift (for each mode type) to map the calculated vibrational frequencies

(21) Li, L.; Fu, Q.; Li, C. H.; Han, B.-K.; Hicks, R. F. *Phys. Rev. B.* **2000**, *61*, 10223.

(22) Frisch, M. J.; Trucks, G. W.; Schlegel, H. B.; Scuseria, G. E.; Robb, M. A.; Cheeseman, J. R.; Zakrzewski, V. G.; Montgomery, J. A.; Stratmann, R. E.; Burant, J. C.; Dapprich, S.; Millam, J. M.; Daniels, A. D.; Kudin, K. N.; Strain, M. C.; Farkas, O.; Tomasi, J.; Barone, V.; Cossi, M.; Cammi, R.; Mennucci, B.; Pomelli, C.; Adamo, C.; Clifford, S.; Ochterski, J.; Petersson, G. A.; Ayala, P. Y.; Cui, Q.; Morokuma, K.; Malick, D. K.; Rabuck, A. D.; Raghavachari, K.; Foresman, J. B.; Cioslowski, J.; Ortiz, J. V.; Stefanov, B. B.; Liu, G.; Liashenko, A.; Piskorz, P.; Komaromi, I.; Gomperts, R.; Martin, R. L.; Fox, D. J.; Keith, T.; Al-Laham, M. A.; Peng, C. Y.; Nanayakkara, A.; Gonzalez, C.; Challacombe, M.; Gill, P. M. W.; Johnson, B. G.; Chen, W.; Wong, M. W.; Andres, J. L.; Head-Gordon, M.; Replogle, E. S.; Pople, J. A. *Gaussian 98*, rev. A.7; Gaussian, Inc.: Pittsburgh, PA, 1998.

Table 1. Comparison of the B3LYP Geometries of In_2H_6

parameters	method		
	this work	ref 11	ref 12
	bond distances (Å)		
In−H^b	1.976	1.946	1.968
In−H^t	1.739	1.710	1.720
In−In	3.020	2.961	3.009
	bond angle (deg)		
∠In−H^b−In (deg)	99.7	99.1	99.7

onto those observed by experiment.[14,29] We have used the same approach here: the predicted In−H stretching frequencies have been uniformly shifted down by 100 cm^{-1} to correct for systematic errors in calculations, due to deficiencies in the cluster models, neglect of anharmonicity, and so forth. This value was derived from the well-defined terminal In−H stretching frequencies seen experimentally (vide infra), and is essentially the same as the values used previously for the Si−H and P−H stretching vibrations.

The accuracy of the calculations was assessed by comparing the M−H stretching frequencies of indane predicted by our method to those predicted with larger basis sets. It was found that the smaller basis sets yielded essentially the same results as the larger ones. For indane, the In−H stretching mode is centered at 1754 cm^{-1}.[9] Our calculation predicted symmetric and asymmetric modes at 1773 and 1777 cm^{-1}, respectively (without applying a correction factor). The relatively small errors for indane suggest that a significant portion of the systematic shift used for the surface frequencies stems from the deficiencies of the cluster models in representing the electronic effects in the real system. For comparison, Hunt et al. obtained frequencies of 1784 and 1818 cm^{-1} for the two modes in indane, employing an uncontracted (7s/6p/2d) valence basis set and a relativistic pseudopotential core for indium.[11] We have also calculated the structure of diindane, and our results are compared to those reported by other research groups in Table 1. In ref 12, the calculations were performed with relativistic small-electron−core pseudopotentials for indium, in which the 28 innermost electrons were described by ECPs and the outer 21 electrons were treated explicitly with an (8s8p5d)/[4s4p3d] contracted basis set. As can be seen from Table 1, excellent agreement is achieved between our calculations and the previously published work.

IV. Results

IV. A. STM Data. A scanning tunneling micrograph of the indium-rich $\delta(2 \times 4)$ surface is shown in Figure 2. This reconstruction exhibits uniform gray rows extending along the $[\bar{1}10]$ crystal axis. Note the presence of a bilayer step in the lower left-hand corner of the image. In the inset, a close up of the surface is shown which highlights the individual $\delta(2 \times 4)$ unit cells (white rectangle). Inside each rectangle, one can discern three bright spots forming an equilateral triangle. This reconstruction is best described by the ball-and-stick model shown in Figure 3.[21,30] A single In−P mixed dimer straddles four In−In dimers located in the next lower layer. In the [110] direction, each set of four indium dimers is separated by a trench.

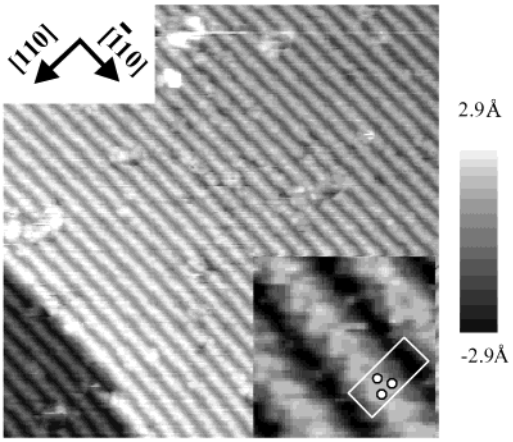

Figure 2. Filled-states STM image of the $\delta(2 \times 4)$ reconstruction (440 × 440 Å^2; (inset) 40 × 40 Å^2).

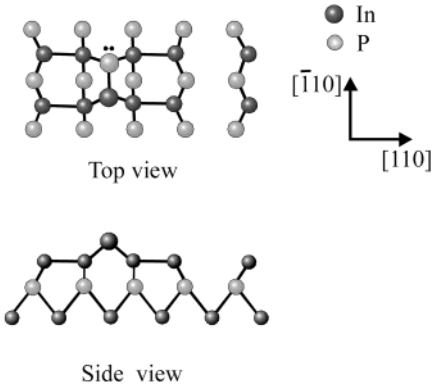

Figure 3. Ball-and-stick model of the $\delta(2 \times 4)$ reconstruction.

The three bright spots seen in the STM image inside each unit cell are due to the filled phosphorus dangling bond and the two In−In back-bonds of each In−P dimer.[31]

IV. B. Vibrational Spectroscopy. Upon dosing the surface with hydrogen, the (2 × 4) LEED pattern gradually converts to (1 × 1), indicating that the hydrogen atoms react with the dimers, breaking some of the In−P and In−In bonds and changing the surface order. Shown in Figure 4 are a series of infrared reflectance spectra for different coverages of hydrogen on the indium-rich $\delta(2 \times 4)$ at 298 K. In these spectra, one sees a series of peaks between 2360 and 2200 cm^{-1} due to P−H stretching modes.[31] In addition, there are two overlapping bands at 1682 and 1660 cm^{-1} attributable to terminal indium hydrides, and two extremely broad bands at about 1350 and 1150 cm^{-1} resulting from bridging indium hydrides. The two terminal hydride bands are resolved upon deconvolution of the infrared spectrum. Saturation of the adsorption sites occurs at about 700 L of H_2, or close to 1.0 L of H atoms. It should be noted that the infrared spectrum cuts off at 1100 cm^{-1} because the lattice vibrations of the crystal absorb all the light in this energy range.

Shown in Figure 5 are polarized infrared reflectance spectra for saturation coverages of hydrogen on the $\delta(2 \times 4)$ reconstruction. The broad bands appearing between 1600 and 1000 cm^{-1} are predominantly p-polarized when light travels along [110] direction (spectrum a), and predominantly s-polarized

(23) Becke, A. D. *J. Chem. Phys.* **1993**, *98*, 1372.
(24) Lee, C. T.; Yang, W. T.; Parr, R. G. *Phys. Rev. B* **1988**, *37*, 785.
(25) Godbout, N.; Salahub, D. R.; Andzelm, J.; Wimmer, E. *Can. J. Chem.* **1992**, *70*, 560.
(26) Igel-Mann, G.; Stoll, H.; Preuss H. *Mol. Phys.* **1988**, *65*, 1321.
(27) Dunning, T. H., Jr.; Hay, P. J. In *Modern Theoretical Chemistry*; Schaefer, H. F., III, Ed.; Plenum: New York, 1976; Vol. 3, p 1.
(28) Bergner, A.; Dolg, M.; Kuechle, W.; Stoll, H.; Preuss, H. *Mol. Phys.* **1993**, *80*, 1431.
(29) Chabal, Y. J. *Surf. Sci. Rep.* **1988**, *8*, 211; Weldon, M. K.; Queeney, K. T.; Gurevich, A. B.; Stefanov B. B.; Chabal, Y. J.; Raghavachari, K. *J. Chem. Phys.* **2000**, *113*, 2440.
(30) Schmidt, W. G. *Phys. Rev. B* **1998**, *57*, 14596.
(31) Hofacker, G. L.; Marechal, Y.; Ratner, M. A. In *The Hydrogen Bond*; Schuster, P., Zundel, G., Sandorfy, S., Eds.; North-Holland: Amsterdam, 1976; Vol. 1, p 294.

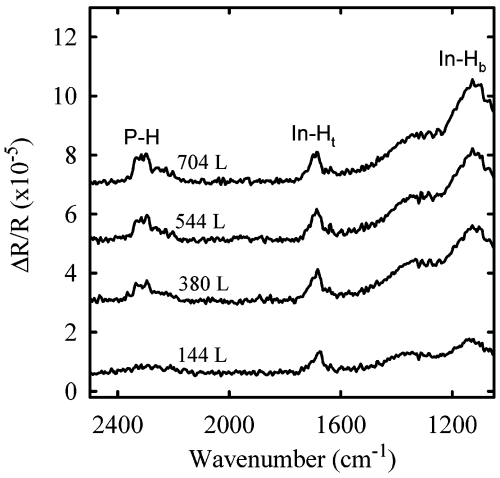

Figure 4. Infrared reflectance spectra of adsorbed hydrogen on $\delta(2 \times 4)$ InP (001) at 25 °C as a function of H_2 dosage.

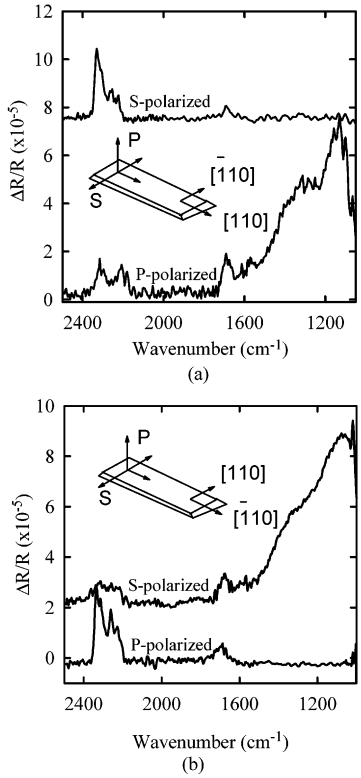

Figure 5. Polarized infrared reflectance spectra of hydrogen adsorbed on the $\delta(2 \times 4)$ surface, with the long crystal axis parallel to (a) the [110] direction and (b) the [1̄10] direction.

when light travels along [1̄10] direction (spectrum b). This indicates that their dipole moments are parallel to [110] crystal axis, which is in the same direction as the indium dimer bond.

IV. C. Ab Initio Calculations. On the $\delta(2 \times 4)$ surface, hydrogen reacts with the indium dimers and either inserts into the In−In bonds or attaches directly to the terminal dangling bonds. Two types of structures that can result from these interactions are represented by clusters **3** and **4** in Figure 6. The molecular cluster **3** simulates the structure of the $\delta(2 \times 4)$ reconstruction whereby one end of each indium dimer is bonded above by the In−P mixed dimer (refer to Figure 3). In cluster **3**, the surface In−In dimer bonds are broken, and two H atoms adsorb onto each indium dimer, one on the terminal site and

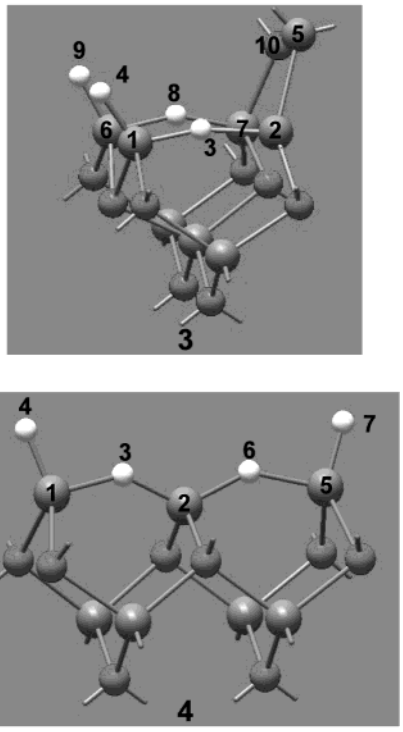

Figure 6. Models of the optimized clusters, showing the indium hydrogen bonds.

Table 2. Vibrational Modes Observed for the Hydrogen-Terminated $\delta(2 \times 4)$ Surface

	theory			experiment	
assignment[b]	frequency (cm^{-1})	intensity	cluster[a]	frequency (cm^{-1})	intensity
In$_1$−H$_4$, In$_6$−H$_9$ (as)	1659	M	**3**	1660	m
In$_1$−H$_4$, In$_6$−H$_9$ (s)	1675	M	**3**	1682	m
In$_1$−H$_4$, In$_5$−H$_7$ (as)	1659	M	**4**	1660	m
In$_1$−H$_4$, In$_5$−H$_7$ (s)	1660	M	**4**	1660	m
In$_1$−H$_3$−In$_2$as	1348	W	**3**	1350	s, br
In$_6$−H$_8$−In$_7$as (as)					
In$_1$−H$_3$−In$_2$as	1384	S	**3**	1350	s, br
In$_6$−H$_8$−In$_7$as (s)					
In$_1$−H$_4$−In$_2$−H$_5$−In$_6$ s	1117	M	**4**	1150	s, br
In$_1$−H$_4$−In$_2$−H$_5$−In$_6$as	1142	S	**4**	1150	s, br
In$_1$−H$_3$−In$_2$s	519	W	**3**	-	
In$_6$−H$_8$−In$_7$s	574	W	**3**	-	
In$_1$−H$_4$−In$_2$−H$_5$−In$_6$ r	436	M	**4**	-	
In$_1$−H$_4$−In$_2$−H$_5$−In$_6$ w	473	M	**4**	-	
In$_1$−H$_4$−In$_2$−H$_5$−In$_6$sc	565	W	**4**	-	

[a] Refer to Figure 6. [b] as = asymmetric; s= symmetric; r =rocking; sc = scissors, w = wag.

one on the bridging site. In cluster **4**, a trimer structure is shown, where two 3c-2e hydride bonds are distributed among three indium atoms. This structure can form whenever one of the In−In dimer bonds is broken on the $\delta(2 \times 4)$ surface (again refer to Figure 3).

The vibrational and geometric properties of the indium hydride clusters are summarized in Tables 2 and 3. The predicted vibrational frequencies are compared to those recorded following hydrogen adsorption on the indium phosphide surface. The isolated terminal indium hydrides on **3** exhibit theoretical stretching modes at 1659 and 1675 cm^{-1}, respectively. The higher-frequency mode has a larger contribution from the hydrogen on the phosphorus side of the In−P mixed dimer. These frequencies are in good agreement with the experimentally observed bands at 1660 and 1682 cm^{-1}. Note that the dipole

Table 3. Bond Lengths (Å) and Bond Angles (deg) for the Indium-Rich Clusters

bond lengths	3	4	bond angles	3	4
$In_1\cdots In_2$	3.915	3.812	$\angle H_4-In_1\cdots H_3$	112.8 ^{o}	96.9^o
In_1-H_3	1.868	2.086	$\angle In_1-H_3-In_2$	165.8 ^{o}	143.0^o
In_2-H_3	2.078	1.933	$\angle H_9-In_6\cdots H_8$	105.7 ^{o}	
In_1-H_4	1.751	1.750	$\angle In_6-H_8-In_7$	156.3 ^{o}	
In_2-In_5	2.876				
$In_6\cdots In_7$	3.816				
In_6-H_8	1.948				
In_7-H_8	1.951				
In_6-H_9	1.749				
In_7-P_{10}	2.611				

moment for this harmonic oscillator has components parallel to the [001] and [110] directions. Due to dielectric screening of the adsorbate layer perpendicular to the surface, the measured intensity along the [001] axis is reduced relative to that along the [110].[18] This is consistent with the measurements of the intensities of the 1660 and 1682 cm^{-1} bands: they are p-polarized when the light is directed down the [110] axis, while they are equally s- and p-polarized when the light is directed down the [$\bar{1}$10] axis. The terminal hydrogen atoms in structure **4** are predicted to occur in the same frequency range.

Hydrogen insertion into the indium dimer bonds produces bridging hydrides as illustrated by clusters **3** and **4** in Figure 6. These species exhibit intense asymmetric stretching modes that are parallel to the [110] axis and very weak symmetric modes that are normal to the surface. As shown in Table 2, the asymmetric stretching vibrations for the bridging hydrides on **3** are predicted to be at 1348 and 1384 cm^{-1}. These modes are about 300 cm^{-1} lower in frequency than the corresponding values for the terminal hydrides. The theoretical results are consistent with the infrared spectrum for the H-$\delta(2 \times 4)$ surface, which contains a broad band located at about 1350 cm^{-1} that is polarized parallel to the [110] direction. On the other hand, the weak symmetric vibrations for the bridging hydrides are predicted to occur at 519 and 574 cm^{-1} and fall below the absorption cutoff for the InP crystal.

In cluster **4**, coupling of adjacent bridged hydrogen atoms occurs, leading to frequency lowering. The coupled symmetric and asymmetric modes are predicted to be at 1117 and 1142 cm^{-1}, respectively. The former vibration with a dipole moment change along the [001] direction is weak in intensity. Conversely, the latter vibration has a strong predicted intensity and a dipole moment change along the [110] direction. We conclude that the intense band observed at 1150 cm^{-1} may be assigned to the asymmetric stretch of the coupled bridging hydride.

V. Discussion

V. A. Vibrational properties. Examination of the infrared spectra presented in Figures 4 and 5 reveals that the bands for the In−H−In species at 1350 and 1150 cm^{-1} are extremely broad. The full-width-at-half-maxima equal 335 and 140 ± 25 cm^{-1}, respectively. A similar broadening has been observed in the infrared spectra of the bridging gallium hydrides on GaAs (001) and in condensed $(GaH_3)_n$ oligomers.[18,19,32] This phenomenon may be attributed to subtle variations in the local chemical environment of the group IIIA elements. On the InP (001) surface, the exposed indium and phosphorus atoms can be coordinated to hydrogen, indium, or phosphorus in a variety of different ways. These alternate configurations will lead to a variation in the distances between the In dimer atoms and the angles of the In−H−In bonds. For example, the molecular clusters **3** and **4** exhibit different equilibrium bond lengths and angles, 3.92 and 3.81 Å, and 166° and 143°, respectively.

Whereas the frequencies for the bridging indium hydride stretching vibrations depend strongly on the local environment, those for the terminal indium hydrides do not. We have investigated this idea to some extent by changing the constraints used in the calculations. In particular, complete relaxation of the doubly bridged $(\mu\text{-H})_2In_3$ structure **4** leads to a large upward shift in the asymmetric stretching frequency. However, this relaxation is unphysical because the second-layer atoms undergo buckling, a motion that is blocked by the extended InP crystal. The vibrational frequencies obtained for the singly bridged structure **3** are less dependent on the constraints. On the other hand, in this compound the frequencies of the bridging hydride modes are affected by the terminal hydrogen bonds. When these are not present, the In−H−In vibrations are shifted lower by 100 to 150 cm^{-1}.

V. B. Bridging Hydride Stability. Bridging indium hydrides are formed on the InP $\delta(2 \times 4)$ reconstruction because the semiconductor lattice creates a template that favors the formation of four-coordinate indium. Moreover, this reaction is driven by the large amount of heat released upon adsorption of hydrogen atoms from the gas phase (for an H atom, $\Delta H_f = 52.2$ kcal/mol).[34] For example, the incorporation of the four hydrogens (two terminal and two bridging) shown in structure **3** involves a reaction enthalpy of −220 kcal/mol. This is similar to the reaction enthalpies for the case of the other group III elements, Al and Ga, which are known to form bridged structures. Thus, one expects to observe bridging hydrides upon H atom adsorption on all the metal-rich III/V compound semiconductor surfaces.

Insertion of hydrogen atoms into the metal dimer bond also releases a substantial amount of strain on the In−P back-bonds. The distance between the two In atoms on the unreconstructed InP (001) surface is 4.2 Å.[35] This may be contrasted to the In−In dimer bond distance, which is calculated to be only 2.9 Å on an optimized cluster **1** without any adsorbed hydrogen. Formation of the 3c-2e bridging bond expands the distance between the indium atoms to approximately 3.8−3.9 Å, a value which is much closer to the surface lattice constant.

Electron transfer between indium and the second-layer phosphorus atoms does not play a role in stabilizing the bridging hydrides. Theoretical calculations of In_2H_6 and $(PH_2)_2In(\mu\text{-H})_2In(PH_2)_2$ using the B3LYP method reveal that the dimerization energy of the latter compound is 5 kcal/mol smaller than that of diindane.[36] In addition, the strain in the surface In−H−

(32) Herzberg, G. *Molecular Spectra and Molecular Structure, Infrared and Raman Spectra of Polyatomic Molecules*; Van Nostrand Reinhold: New York, 1945; Vol. 2, p 168.

(33) Kerr, J. A. In *CRC Handbook of Chemistry and Physics 1999−2000: A Ready-Reference Book of Chemical and Physical Data*, 79th ed.; Lide, D. R., Ed.; CRC Press: Boca Raton, Florida, 1998.

(34) Swaminathan, V.; Macrander, A. T. *Material Aspects of GaAs and InP Based Structures*; Prentice Hall: Englewood Cliffs, NJ, 1991.

(35) The dimerization energy of $(PH_2)_2In(\mu\text{-H})_2In(PH_2)_2$ is calculated relative to the energy of $(PH_2)_2InH$ according to the following reaction: $2(PH_2)_2InH \rightarrow (PH_2)_2In(\mu\text{-H})_2In(PH_2)_2$.

(36) The P−H, In−H and In−In bond energies are assumed to equal 76, 58 and 24 kcal/mol, respectively (Ref. *34*). The former value was estimated from the heat of formation of phosphine, whereas the latter two values were taken from the single bond energies listed in ref 1, p 2.

In bond formed by hydrogen adsorption on the $\delta(2 \times 4)$ reconstruction makes the bridging bond somewhat weaker than in diindane. In the former case, the indium atoms are pulled apart by their back-bonds to phosphorus. Examination of Tables 1 and 3 reveals that the In−In bond distances and In−H−In bond angles are 3.0 Å and 100° in In_2H_6, compared to 3.8 Å and ∼160° in cluster **3**. Finally, it is interesting to note that the vibrational frequencies of the terminal indium hydrides on H:InP (001) are significantly lower than those of InH_3.

VI. Conclusions

This work demonstrates that the $\delta(2 \times 4)$ reconstruction of indium phosphide provides a unique environment for investigating the reactivity of atomic hydrogen (and other ligands) toward the electron-deficient indium atoms. Terminal and bridging hydrides are formed at room temperature, with vibrational frequencies occurring at 1660−1682 and 1350−1150 cm^{-1}, respectively. The 3c-2e bonds are actually weaker on the surface than in the gas phase, owing to the strained back-bonds between the indium dimers and the underlying phosphorus atoms. Nevertheless, we may now add indium to the list of group IIIA elements that are known to form covalent bridging hydride bonds.

Acknowledgment. Funding for this research was provided by the National Science Foundation, Divisions of Chemical and Transport Systems and Materials Research.

JA020348P

(37) Here, $\Delta E^{298}_{In-H-In} = {}^1/_2\Delta E^{298}_{rxn} + \Delta E^{298}_{In-H}$, where the second term equals the dimerization energy, 22 kcal/mol, and the last term is 58 kcal/mol (ref 1, p 12).